A Simple Theory of Optimal Coherent Control

Ruixue Xu, Jixin Cheng, and YiJing Yan*

Department of Chemistry, Hong Kong University of Science and Technology, Kowloon, Hong Kong, and Open Laboratory of Bond-Selective Chemistry, University of Science and Technology of China, Hefei, China

Received: June 15, 1999; In Final Form: September 7, 1999

By combining the theories of optimal control and coherent control, we derive an analytical formulation to evaluate the optimal 1-photon and *n*-photon fields together with their relative phase and intensity in the optimal "1 + *n*"-coherent control scheme. The optimal coherent control exploits tailored light pulses to produce the best overlap with a predefined nuclear target in an electronically degenerate region. It also exploits explicitly the quantum interference between two optimal excitation pathways to achieve the product electronic selectivity. Numerical demonstrations are carried out to selectively control a minimum-uncertainty outgoing wave packet target in a molecular system. The electronically degenerate byproduct is shown to be completely discriminated against via the destructive interference between two optimal excitation pathways. The target considered in this paper would neither be achievable via the conventional continuous-wave coherent control nor via a single optimal control pathway in the weak response regime. Proposed is also a time-dependent excitation frequency degeneracy condition that incorporates the evolution of carrier frequencies in the optimal coherent control with tailored light fields.

I. Introduction

In recent years rapid progress in the use of tailored light to actively guide chemical and molecular events has occurred. Kent R. Wilson, to whom this issue of *The Journal of Physical Chemistry A* is dedicated, has been one the most active advocates of this scientific endeavor. His concerted research activities toward the goal of controlling chemical dynamics range from the development of fundamental theories,[1−6] technology,[7−9] and experiments,[10−14] together with the staging of his state-of-the-art multimedia seminars. One of us (Y.J.Y.) fortunately participated in the early phase of the joint theory−experiment effort in "Kent R. Wilson's La Jolla school" with the goal of realizing the manipulation of molecular dynamics by light.

Generally speaking, there are two active control approaches that use the coherent property of light to manipulate molecular or chemical dynamics.[15] One approach is based on the coherent control theory (CCT) originally proposed by Brumer and Shapiro.[16,17] In CCT the chemical selectivity is controlled as a direct consequence of quantum interference. One of the representative coherent control scenarios is the interference between one- and three-photon pathways, both of which connect the initial bound state of reactant to a degenerate doorway to two different products in a continuum.[16−19] It has been shown that the product selectivity can be controlled by varying the relative phases and amplitudes of multiple independent but degenerate excitation pathways.[16−19] The coherent control scheme has been demonstrated experimentally in a variety of atomic and molecular systems.[20−29]

An alternative approach of active control is to design tailored light pulses or pulse trains to drive reactions to the desired products.[1−4,30−44] The foundation of this approach is the optimal control theory (OCT) employed first by Rabitz and co-workers.[34−36] Extension of OCT to molecular systems with multiple electronic surfaces was made by Kosloff et al.,[33] and to condensed phases by Wilson and co-workers.[1] Recently, Yan and co-workers have further extended OCT to the multiple phase-unlocked control fields, such as in the case of pump−dump or pump−pump processes.[45−50] Successful experiments in optimal control are now emerging rapidly.[10−14,51−53] Recent development involves a combination of the pulse shaping techniques[54−56] and automated control feedback loops.[57−59] The adaptive feedback optimal control scheme uses the dynamic signals of molecular system to teach the pulse shaping apparatus to generate the improved field as it drives the molecule toward the desired target.[14,53]

In general, OCT results in a nonlinear equation whose solution can only be solved in an iterative manner. The converged control field is only locally optimal and depends usually on the input to initiate the iteration procedure. While it is transparent in CCT, the quantum interference among various excitation pathways is often obscure in OCT. Mathematically, OCT is a problem of optimization in a functional space, and CCT is in a parameter space. In this sense, one may view CCT as a special case of OCT with certain appropriate constraints such as the shapes of control fields with specific quantum interference scheme. Paramonov and Manz and their co-workers[37−40] have described a parameter−space control scheme using pulse sequence in which the duration, intensity, frequency, and time delay of each pulse are optimized. Recently, Gross and Rabitz[60] have further pointed out that the coherent control based on a specific quantum interference scheme can also be more generally formulated in terms of optimization in parameter space.

In this paper, we shall present an optimal coherent control (OCC) scheme which coherently combines the OCT for the individual one-photon and multiphoton excitation processes in the weak response regime. The control scenario may be schematically represented in Figure 1. The molecule is initially

* To whom correspondence should be addressed. E-mail: yyan@ust.hk.

10.1021/jp991965b CCC: $18.00
Published on Web 11/18/1999

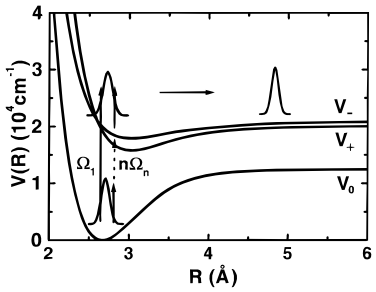

Figure 1. Schematic diagram of control in a model molecular system via one-photon and multiphoton excitation pathways either individually or in the "1+*n*"-interference manner. The two excited states $|+\rangle$ and $|-\rangle$ are degenerate with same optical selection rules.

in the ground $|0\rangle$ surface (or reactant), and the target is an excited $|+\rangle$ species (or product) with a specific form such as a minimum uncertainty wave packet in the nuclear phase-space. It is well established that the optimal control field to this target should be properly shaped.[2] However, when the undesired byproduct $|-\rangle$ state with the same optical selection rule is degenerate with the product $|+\rangle$ state, the chemical selectivity is neither achievable in a one-photon nor a multiphoton process individually in the weak response regime. The standard approach in OCT is to iteratively solve the nonlinear equation in the strong response regime. The resulting field contains usually multiple phase-locked subpulses, involving various competitive processes such as dynamic Stark shift, power broadening, multiphoton absorption, and ionization. The OCC scheme proposed in this paper explicitly exploits the quantum interference between two optimally tailored, e.g., one- and three-photon excitation pathways. The relative phase and intensity between the one- and three-photon control fields together with their optimal time-frequency shapes will thus be determined. The OCC theory provides a clear physical picture of the control processes in terms of light-matter interference in both phase-amplitude[16−19] and time-frequency[1−3,32−36] spaces. The remainder of this paper is organized as follows. In section II, we develop a simple theory of optimal coherent control via the interference between two optimal photon excitation pathways. In section III, we present numerical demonstrations in a molecular system for controlling a localized wave packet with a predefined product electronic selectivity. Finally, we summarize and conclude this work in section IV.

II. Theory

A. A Simple Theory of Multiphoton Control. In this section, we shall develop a simple theory of optimal coherent control that consists of two parts. The first part that will be presented in the following deals with the optimal multiphoton control. The second part that will be discussed in the next subsection considers the quantum interference between two optimal photon excitation pathways.

Let us consider the simplest *n*-photon excitation control in a molecular system in which there are no resonant intermediates to assist the multiphoton process (cf. Figure 1). The molecule is assumed to be initially in a nuclear eigenlevel, $\psi(0) = |\nu''\rangle$, of the ground electronic state labeled as "0". The control target is a pure state $|\phi_e\rangle$ that describes a nuclear wave packet on the doubly degenerate electronic excited state involving both/either "+" and/or "−" electronic surfaces (cf. Figure 1). For simplifying the notation, we set the energy zero as $\epsilon_{\nu''} = 0$ and $\hbar = 1$.

In the presence of an *n*-photon excitation field, the molecule is excited onto the degenerate excited state surfaces. We shall denote the carrier frequency and the slowly varying complex amplitude of the *n*-photon excitation field as Ω_n and $E_n(t)$, respectively. In the system of study, the field-matter interaction can be described by

$$H'(t) = e^{-in\Omega_n t}\hat{\alpha}^{(n)}E_n^n(t)|e\rangle\langle 0| + H.c. \tag{1}$$

H.c. denotes the Hermitian conjugate, while $|e\rangle = \{|+\rangle, |-\rangle\}$ is the degenerate electronic excited state. In eq 1, $\hat{\alpha}^{(n)}$ is the molecular polarizability operator for the *n*-photon absorption process. In the case of one-photon excitation, $\hat{\alpha}^{(1)} \equiv \hat{\mu}$ assumes the electronic transition dipole operator. The molecular wave packet excited by the *n*-photon process is then described by

$$|\psi_e^{(n)}(t)\rangle = e^{-in\Omega_n t}\int_0^t d\tau\, E_n^n(\tau)|\psi'^{(n)}_e(t-\tau)\rangle \tag{2}$$

Physically, $\psi'^{(n)}_e(\tau)$ in eq 2 can be considered as the molecular "bare" wave packet excited via an impulsive *n*-photon excitation field in the electronic rotating wave approximation. $\psi'^{(n)}_e(\tau)$ is purely a property of matter and given formally by

$$|\psi'^{(n)}_e(\tau)\rangle = e^{-iH_e\tau}\hat{\alpha}^{(n)}|\nu''\rangle \tag{3}$$

Here, H_e is the Hamiltonian operator governing molecular dynamics in the degenerate excited state involving both the "+" and "−" electronic surfaces (cf. Figure 1).

The goal of control is to find the *n*-photon field $E_n(t)$ that optimally drives the molecular system $\psi_e^{(n)}(t_f)$ to the desired target state ϕ_e at a chosen target time t_f under certain constraints that will be specified later. The time-dependent target expectation value is given by

$$|c_n(t)|^2 \equiv |\langle\phi_e|\psi_e^{(n)}(t)\rangle|^2 \tag{4}$$

Here, $c_n(t)$ is the *n*-photon control amplitude which in general is complex. At any given target time t_f it is given by

$$c_n(t_f) = e^{-in\Omega_n t_f}\int_0^{t_f} dt\, E_n^n(t)\langle\phi_e|\psi'^{(n)}_e(t_f - t)\rangle \tag{5}$$

For the clarity of theoretical formalism, we introduce in this paper an *n*-photon scaled field intensity defined as

$$I_n = \int_0^{t_f} dt\, |E_n(t)|^{2n} \tag{6}$$

Obviously, the *n*-photon control yield $|c_n(t_f)|^2 \propto I_n$. The control objective can then be described as to find the *n*-photon excitation field $E_n(t)$ that optimizes the control yield $|c_n(t_f)|^2$ at a given finite value of I_n. By using the Lagrange λ-multiplier method, the problem of *n*-photon control can thus be cast as the optimization of the following control objective functional,

$$J(t_f) = |c_n(t_f)|^2 - \lambda_n I_n \tag{7}$$

We shall therefore consider the variation of the control functional $J(t_f)$ with respect to $\delta E_n(t)$, the variation in the control field E_n.

$$\delta J(t_f) = c_n^*(t_f)\delta c_n(t_f) - \lambda_n \delta I_n \tag{8}$$

The asterisk "∗" denotes the complex conjugate. From eqs 5 and 6, we have

$$\delta c_n(t_f) = n e^{-in\Omega_n t_f}\int_0^t dt\langle\phi_e|\psi'^{(n)}_e(t_f - t)\rangle E_n^{n-1}(t)\delta E_n(t) \tag{9}$$

$$\delta I_n = n\int_0^{t_f} \mathrm{d}t[E_n^*(t)]^n E_n^{n-1}(t)\delta E_n(t) \tag{10}$$

By using the variation principle $\delta J(t_f) = 0$, we thus obtain the following solution to the n-photon control field in the weak response regime,

$$\tilde{c}_n^*(t_f)\langle\phi_e|\psi'^{(n)}_e(t_f - t)\rangle = \lambda_n[E_n^*(t)]^n \tag{11}$$

Here,

$$\tilde{c}(t_f) \equiv \mathrm{e}^{in\Omega_n t_f} c_n(t_f) \tag{12}$$

is the control amplitude (cf. eq 5) with the removal of the electronic phase. Obviously, eq 11 is the extension of one-photon control formulation[30,50] to the simple n-photon scenario considered in this paper. Note that there is an arbitrary phase associating with the control amplitude. In this paper, we shall set $\tilde{c}_n(t_f)$ to be *real* and *positive*. Moreover, we can show from eqs 5 and 6 that the Lagrange multiplier relates to the control yield as $\lambda_n = |c_n(t_f)|^2/I_n$. The final equation for the optimal n-photon control can thus be written as

$$\langle\phi_e|\psi'^{(n)}_e(t_f - t)\rangle^* = \frac{|c_n(t_f)|}{I_n} E_n^n(t) \tag{13}$$

The quantity on the left-hand-side of the above equation depends only on the matter and the target, but not on the external driving field. Equation 13 is the direct extension of one-photon control[30,50] to the solution of the optimal n-photon field $E_n(t)$ in the present system of study. It is easy to show that by using the optimal n-photon control field in eq 13 the control amplitude $\tilde{c}_n(t_f)$ evaluated via eqs 5 and 12 is real and positive. This result is consistent with our choice of phase zero, $\arg[\tilde{c}_n(t_f)] = 0$. This phase property will also be important in the development of optimal coherent control theory to be presented in the next subsection.

Note that eq 13 may be simplified as $E_n^n(t) \propto \langle\phi_e|\psi'^{(n)}_e(t_f - t)\rangle^*$ if only the single excitation pathway is considered. The absolute intensity of single n-photon field provides only a power-law scaling factor in the weak response regime. A single optimal n-photon control pathway would excite the wave packet onto both the excited product $|+\rangle$ and the byproduct $|-\rangle$ states. We shall in the next subsection consider the product selectivity control via the coherent superposition of two optimal optical excitation pathways (cf. Figure 1). In this case, not only the phase $\arg[\tilde{c}_n(t_f)]$ (cf. eq 13 and its comments followed) but also the amplitude $|c_n(t_f)|$ will play important roles. The prefactor to the field in eq 13 can then be used to relate the control yield $|c_n(t_f)|^2$ to the incident n-photon scaled intensity I_n (eq 6); that is,

$$|c_n(t_f)|^2 = I_n\int_0^{t_f} |\langle\phi_e|\psi'^{(n)}_e(t_f - t)|^2 \mathrm{d}t \tag{14}$$

The above equation will be used to determine the relative intensities of multiple excitation pathways (cf. eq 20) in the optimal coherent control, allowing a discrimination against the degenerate byproduct.

B. A Simple Theory of Optimal Coherent Control. We shall now complete the optimal coherent control theory by considering the coherent superposition of two independent photon excitation pathways. Without losing the generality, we consider one excitation pathway is the one-photon control and another is an n-photon ($n > 1$) process. The total field in the optimal coherent control assumes the following form:

$$\epsilon_T(t) = E_1(t)\mathrm{e}^{-i(\Omega_1 t+\theta)} + E_n(t)\mathrm{e}^{-i\Omega_n t} + c.c. \tag{15}$$

Here, θ is the additional phase that determines the nature of coherent control. We shall discuss this issue later.

In order to achieve the maximum interference between two optical control pathways, the carrier frequencies should satisfy the degeneracy condition,

$$n\Omega_n = \Omega_1 \tag{16}$$

while the control amplitudes should be equal

$$c = |c_1(t_f)| = |c_n(t_f)| \tag{17}$$

The optimal shapes of both the one-photon control field $E_1(t)$ and the n-photon control field $E_n(t)$, together with their relative intensity, are given by eq 13. We obtain

$$E_1(t) \propto \langle\phi_e|\psi'^{(1)}_e(t_f - t)\rangle^* \tag{18}$$

$$E_n^n(t) \propto \langle\phi_e|\psi'^{(n)}_e(t_f - t)\rangle^* \tag{19}$$

Each of the above equations differs from eq 13 only by a positive prefactor. The above equations thus determine the optimal $E_1(t)$ and $E_n(t)$ fields together with their relative phase. Their relative intensity can be obtained by using eqs 14 and 17, resulting in

$$\frac{I_1}{I_n} = \frac{\int_0^{t_f} |\langle\phi_e|\psi'^{(n)}_e(t_f - t)\rangle|^2 \mathrm{d}t}{\int_0^{t_f} |\langle\phi_e|\psi'^{(n)}_e(t_f - t)\rangle|^2 \mathrm{d}t} \tag{20}$$

In eq 15, θ is an additional adjustable phase parameter to regulate the total yield of optimal coherent control. As we mentioned following eq 13, in the absence of the additional phase, i.e., $\theta = 0$, the phase difference between the control amplitudes was given by $\arg[c_1(t_f)] - \arg[c_n(t_f)] = (\Omega_1 - n\Omega_n)t_f$, which is zero under the degeneracy condition (eq 16). By introducing an additional phase θ and under the maximum interference condition (eq 17), the optimal "1 + n"-coherent control yield is then given by

$$|c_T(t_f)|^2 = |c_1(t_f) + c_n(t_f)|^2 = 4|c|^2 \cos^2(\theta/2) \tag{21}$$

Equations 15−21 together with eq 3 constitute the final formulation for the optimal "1 + n"-coherent control of molecular systems in which there are no other resonant surfaces between the initial and the final target states. The optimal coherent control enables not only the maximum enhancement of the target yield in the product electronic $|+\rangle$ state by setting $\theta = 0$, but also the maximum elimination of the byproduct in the $|-\rangle$ state by setting $\theta = \pi$. In the latter case, the target maybe chosen as of the same nuclear wave packet but in the electronic $|-\rangle$ state (cf. Figure 1). It is easy to show that in the case of eigenstate control, the present theory recovers the well established "1 + n" continuous-wave coherent control formalism.[16−19]

III. Numerical Results and Discussions

For the numerical demonstration of optimal coherent control, we consider a model molecular system of three Morse potential surfaces (Figure 1) whose parameters are listed in Table 1. The reduced molecular mass is set to be $m = 64$ amu. The molecule is initially at the $v'' = 0$ vibronic level in the ground $|0\rangle$ electronic state. Its eigenenergy is 107.0 cm^{-1} above the potential minimum. We shall consider the control of a minimum

TABLE 1: Parameters for the Potential Surfaces: $V(R) = T_e + D_e[1 - e^{-\beta(R-R_e)}]^2$

	T_e (cm^{-1})	D_e (cm^{-1})	β (Å^{-1})	R_e (Å)
V_0	0	12550	1.871	2.666
V_+	15769	4381	1.876	3.016
V_-	17097	3000	1.876	3.016

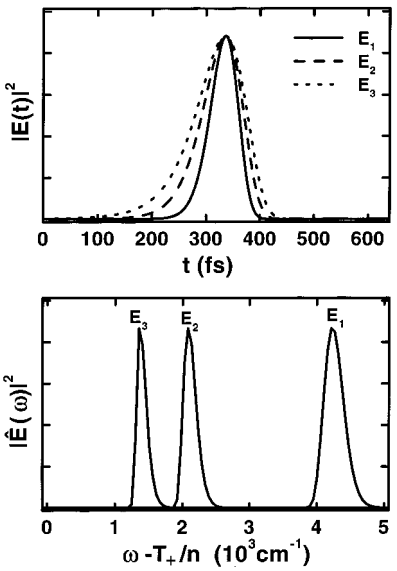

Figure 2. The temporal (upper part) and the spectral (lower part) profiles of the optimal one-photon (E_1), two-photon (E_2), and three-photon (E_3) excitation fields. Their peak powers are 8.14×10^9, 3.06×10^{11}, and 3.24×10^{12} W/cm^2, respectively (see text). The control target is an outgoing minimum-uncertainty Gaussian wave packet in the $|+\rangle$ state (see text). The potential minimum (T_e) of the $|+\rangle$ state is $T_+ = 15769$ cm^{-1}. The target time is 640 fs.

uncertainty Gaussian wave packet in the excited $|+\rangle$ state; i.e. $\phi_e = \phi_+|+\rangle$ with

$$\phi_+(R) = (2\pi\Delta_r^2)^{-1/4} e^{-(R-\bar{r})^2/(4\Delta_r^2) - i\bar{p}(R-\bar{r})/\hbar} \tag{22}$$

Here, $\bar{r}$ and $\bar{p}$ are the position and the momentum centers, respectively, while Δ_r is the variance in position. The coherent state target in eq 22 satisfies the minimum uncertainty relation: $\Delta_r\Delta_p = \hbar/2$. In the following calculation, we choose $\bar{r} = 4.8$ Å, $\Delta_r = 0.166$ Å, and a mean outgoing momentum $\bar{p} > 0$ that corresponds to a kinetic energy of $\bar{p}^2/(2m) = 400$ cm^{-1}. The mean vibronic energy of this target is about 4411 cm^{-1} above the potential-zero of the $|+\rangle$ target surface. As the initial wave packet in the $|0\rangle$ state is 107 cm^{-1} above the potential minimum, it would be expected that the carrier frequency of the n-photon control field ($n = 1$, 2, or 3) is around $\Omega_n = (T_+ - 107.0 + 4411.4)/n$ cm^{-1} $= (T_+ + 4304.4)/n$ cm^{-1} (cf. Figure 2). Here, $T_+ = 15769$ cm^{-1} is the frequency difference between the potential minimum (i.e., T_e) of the target $|+\rangle$ state and that of the initial ground $|0\rangle$ surface (cf. Table 1). The target time is chosen to be $t_f = 640$ fs.

For the purpose of comparison, we assume there is no symmetry restriction. Each of the individual one-photon, two-photon, or three-photon processes can excite the initial wave packet in the ground $|0\rangle$ state to both of the electronically degenerate states, $|+\rangle$ and $|-\rangle$. For simplicity, we neglect the effects of nonadiabatic coupling and rotation. The transition dipoles/polarizabilities are chosen such that $\mu_+ = -\mu_- =$ constant for the one-photon, $\alpha_+^{(2)} = \alpha_-^{(2)} \propto \exp(R)$ for the two-photon, and $\alpha_+^{(3)} = \alpha_-^{(3)} \propto \exp(2R)$ for the three-photon absorption processes. Their magnitudes in the experimental units will be exemplified later in the discussion of the scaling law of the control yield (cf. eq 26).

To measure the quality of a control field, we also calculate the achievement function defined as[2,3]

$$a(t) = \frac{|\langle\phi_+|\psi_+(t)\rangle|}{\sqrt{\langle\phi_+|\phi_+\rangle\langle\psi_+(t_f)|\psi_+(t_f)\rangle}} \tag{23}$$

Obviously, $0 \le a(t_f) \le 1$. The perfect control may be referred to the case of $a(t_f) = 1$ at the target time. Note $a(t_f)$ is a normalized measure at t_f for the overlap between the controlled wave packet and the target. It provides no information on whether there is byproduct or not. As to be demonstrated numerically, each of the individual optimal excitation pathways generates an excited wave packet that nearly 100% matches with the predefined target in the product $|+\rangle$ electronic state at the specified target time t_f. However, none of them alone is able to eliminate the byproduct in the degenerate $|-\rangle$ state. The optimal coherent control theory developed in section II B will be shown to be capable of not only a constructive enhancement of product yield but also a destructive elimination of the degenerate byproduct.

Figure 2 depicts the temporal (upper part) and spectral (lower part) profiles of the optimal one-, two-, and three-photon control fields. Their temporal peaks are all near 330 fs. Each of their center frequencies is around the intuitively estimated value of $\Omega_n/(\text{cm}^{-1}) = (T_+ + 4304.4)/n$. The final achievement $a(t_f)$ (cf. eq 23) for the optimal one-, two-, and three-photon controls are 0.98, 0.97, and 0.97, respectively. All these three optimal fields are of simple forms, and can be well represented by chirped Gaussian pulses. Together with the carrier frequency (cf. eq 15), we fit the control field as

$$E_n(t)e^{-i\Omega_n t} = \sqrt{A_n}e^{-(t-\bar{t}_n)^2/(2\Gamma_n^2)}e^{-i\varphi_n(t-\bar{t}_n)} \tag{24}$$

with

$$\varphi_n(t) = \varphi_n^{(0)} + \Omega_n t + \frac{1}{2}c_n' t^2 + \frac{1}{6}c_n'' t^3 \tag{25}$$

Each Gaussian pulse field is characterized by seven parameters, the peak power A_n, temporal center $\bar{t}_n$, temporal variance Γ_n, constant phase $\varphi_n^{(0)}$, the carrier frequency Ω_n, linear temporal chirp c_n', and quadratic chirp c_n'', respectively.

As we mentioned earlier, the absolute value of peak power A_n and constant phase $\varphi_n^{(0)}$ would not be well-defined in the optimal control theory that employs an individual optical excitation pathway in the weak response regime. However, the relative peak power, or more precisely the relative intensity (eq 20 with eq 6), and the relative phase play crucial roles in an optimal coherent control scheme in which multiple degenerate excitation pathways interfere with each other. We can evaluate the constant phases via $\varphi_n^{(0)} = \varphi_n(t{=}0)$ (cf. eq 25) and the relative scaled intensities via eq 20. For a given shape of control field, the control yield scales with the peak power and the dipole/polarizability magnitude as (cf. eq 14 with eq 3)

$$|c_n(t_f)|^2 \propto |\alpha^{(n)}|^2 A_n^n \tag{26}$$

In order to specify the peak power A_n in an experimental unit, we choose the transition dipoles/polarizabilities for the model molecular system at its ground electronic state minimum as $\mu_\pm = \pm 1$ Debye, $\alpha_\pm^{(2)} = 10^{-27}$ m^3, and $\alpha_\pm^{(3)} = 10^{-37}$ m^3 (V/m)$^{-1}$. These values are of reasonable magnitude for molecules of

TABLE 2: Best-Fit Gaussian Pulse Parameters for the Optimal One-, Two-, and Three-Photon Excitation Fields

	one-photon	two-photon	three-photon
$\bar{t}_n$ (fs)	329.8	322.6	314.7
Γ_n (fs)	37.57	55.10	70.21
Ω_n (cm^{-1})	20025	9999	6657
$\varphi_n^{(0)}$	−1.40	−0.70	−0.47
c_n' (cm^{-1}/fs)	4.174	1.966	1.223
c_n'' (cm^{-1}/fs^2)	0.039	0.0171	0.0102

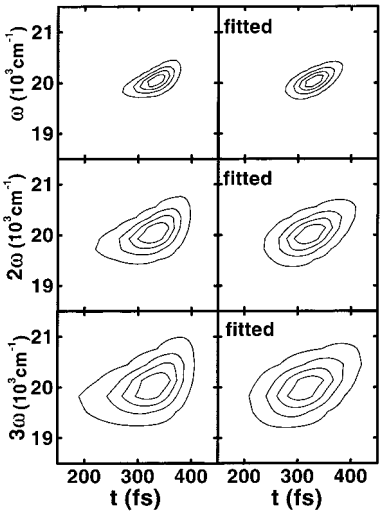

Figure 3. Wigner spectrograms of the optimal one-photon (upper), two-photon (middle), and three-photon (bottom) excitation fields in Figure 2. The best-fit Gaussian fields are presented in the right.

moderate to large size. The control yield at the target time is chosen to be $|c_n(t_f)|^2 = |\langle\phi_+|\psi_+^{(n)}(t_f)\rangle|^2 = 0.02$ for each individual optimal excitation pathway. As a nearly perfect control [cf. eq 23 with $a(t_f) \approx 1$] at the target time t_f, the transferred population into the $|+\rangle$ state, $P_+(t_f) \equiv \langle\phi_+^{(n)}(t_f)|\phi_+^{(n)}(t_f)\rangle = |c_n(t_f)|^2/a^2(t_f)$, will also be about 2% in each individual optimal excitation pathway. For the above given values of dipole/polarizabilities and control yield, the resulting peak powers are $A_1 = 8.14 \times 10^9$ W/cm^2, $A_2 = 3.06 \times 10^{11}$ W/cm^2, and $A_3 = 3.24 \times 10^{12}$ W/cm^2 in the optimal one-, two-, and three-photon control processes, respectively.

Listed in Table 2 are the other best-fit Gaussian parameters in eq 24 with 25 for each individual optimal field. The temporal center $\bar{t}_n$ is found to be about the same in each field. However, the temporal width of control field Γ_n scales as $\sim\sqrt{n}$, the square root of photon number (cf. the upper panel of Figure 2). This result is consistent with eq 19. Correspondingly, the spectral width of the control field decreases as the photon number n increases (cf. the lower panel of Figure 2).

The time-dependent phase $\varphi_n(t)$ (eq 25) that describes the coherent time-frequency property of the optimal field plays a crucial role in the control of molecular dynamics.[2,3,10−13,53] Figure 3 presents the Wigner spectrograms of individual optimal fields (left part) and their best-fit Gaussian counterparts (eqs 24 and 25 with Table 2). This figure provides thus a graphical visualization of the time-frequency coherence in each optimal field as well as its fitness into a simple Gaussian pulse. The optimal chirps are mainly linear. They are all positive, favoring the focused outgoing target.[2,3] It is interesting to notice that besides the optimal carrier frequency of n-photon field satisfying $n\Omega_n \approx \Omega_1$ (cf. eq 16), the optimal zero-phase and linear chirp also follow the similar relations, $n\varphi_n^{(0)} \approx \varphi_1^{(0)}$ and $nc_n' \approx c_1'$ (cf. Table 2). These results together may suggest the extension of

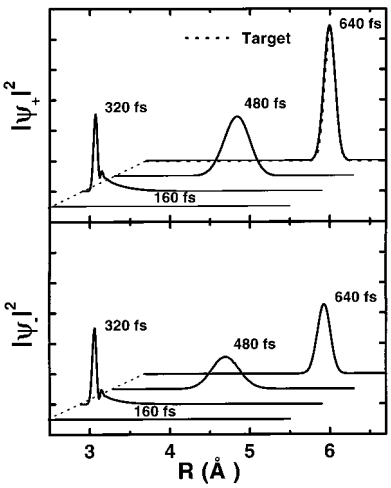

Figure 4. Wave packet evolution on the two degenerate $|+\rangle$ and $|-\rangle$ state surfaces via the optimal one-photon control. The wave packet dynamics controlled individually by the optimal two- or three-photon field behave similarly. The target is also depicted (dotted) to demonstrate the control quality.

the degenerate excitation frequency (eq 16) to the *degenerate time-frequency coherence* condition (cf. eq 25):

$$n\varphi_n(t) = \varphi_1(t) \tag{27}$$

for the optimal "1 + n"-coherent control.

To proceed, let us first use the obtained optimal/best-fit fields individually to numerically propagate wave packets on both of the two degenerate excited $|+\rangle$ and $|-\rangle$ surfaces. Figure 4 shows the resulting wave packet evolutions that are essentially the same in either the one-, two-, or three-photon processes, and in either the optimal or the best-fit Gaussian fields, individually. At the target time of $t_f = 640$ fs, the controlled wave packet $\psi_+(t_f)$ overlaps almost perfectly with the predefined target (dotted curve in the upper part of Figure 4). It indicates that a nearly perfect control $a(t_f) \approx 1$ in terms of normalized achievement (cf. eq 23) can be accomplished by each of these three optimal excitation pathways. However, the control with a single optimal excitation pathway generates also a significant amount of the $|-\rangle$ electronic state byproduct (cf. the lower part of Figure 4).

We now turn to the results of optimal coherent control (OCC) based on the formulation developed in section II B. On the top of achieving a nearly perfect normalized wave packet−target overlap, $a(t_f) \approx 1$, the OCC is also able to control over the product selectivity in either the $|+\rangle$ or the $|-\rangle$ states. Without losing the generality, we shall in the following present the results of optimal "1+3" coherent control. Note the optimal one-photon and three-photon fields obtained previously have been locked with each other in both of their phases and intensities. The resulting control amplitudes satisfy the relations of $\arg[c_1(t_f)] = \arg[c_3(t_f)]$ and $|c_1(t_f)| = |c_3(t_f)|$. Therefore, the additional relative phase θ (cf. eq 15) to the calculated optimal one-photon pathway regulates the yield (amplitude square) of optimal "1+3"-coherent control (cf. eq 21). The physical origin of the product selectivity lies on the molecular phase difference between the $|+\rangle \leftarrow |0\rangle$ and $|-\rangle \leftarrow |0\rangle$ transitions associated with the "1+3"-coherent control scheme.

Figure 5 depicts the evolution of wave packets under the optimal coherent "1+3" control without the additional phase, $\theta = 0$. While it remains a nearly perfect overlap with the target in terms of the normalized achievement $a(t_f) \approx 1$, the selectivity on the $|+\rangle$ product is also achieved via an almost perfectly destructive interference against the $|-\rangle$ byproduct. In comparison

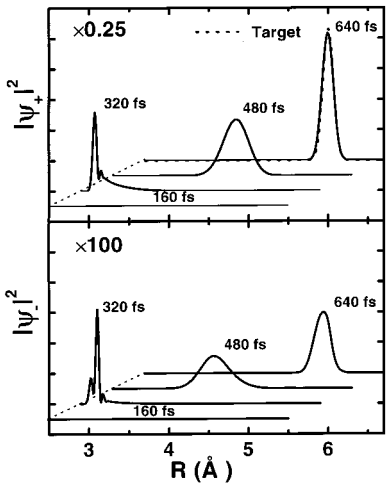

Figure 5. Wave packet evolution on the two degenerate $|+\rangle$ and $|-\rangle$ state surfaces via the optimal "1+3"-coherent control. The additional phase $\theta = 0$.

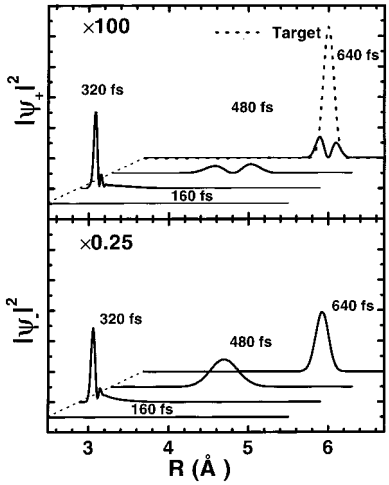

Figure 6. Same as Figure 5 but with $\theta = \pi$.

with the individual optimal one- or three-photon process (cf. Figure 4), the yield of $|+\rangle$ product is quadrupled, while that of $|-\rangle$ byproduct decreases by more than two orders of magnitude. Note that the setting of $\theta = 0$ is designed for the constructive maximization of the $|+\rangle$ product rather than the destructive minimization of the $|-\rangle$ byproduct. However, the transition dipoles/polarizabilities have been chosen as $\mu_- = -\mu_+$ for the one-photon excitation and $\alpha_-^{(3)} = \alpha_+^{(3)}$ for three-photon pathway. The electronic contribution to the molecular phase difference between the "1+3"-control of $|+\rangle$ and $|-\rangle$ states has the value of π. For the molecular system in study, the nuclear contribution to the matter phase difference is relatively small. As a result, in the optimal "1 + 3"-coherent control with $\theta = 0$ in which the $|+\rangle$ product yield is constructively maximized, the $|-\rangle$ byproduct yield is about destructively minimized. In the optimal coherent control scenario, the maximal discrimination against the $|-\rangle$ byproduct should in general be done by defining a suitable target in the $|-\rangle$ state and then setting $\theta = \pi$ (cf. eq 21 and its comments). In this case, the product branching ratio P_+/P_- is usually maximized, but the target achievement $a(t_f)$ and the control yield $|c_T(t_f)|^2$ in the product $|+\rangle$ state may decrease.

Figure 6 shows the evolution of wave packets under the optimal coherent "1+3" control with the additional phase of $\theta = \pi$. In this case, the control yield $|c_T(t_f)|^2$ and the population $P_+(t_f)$ in the $|+\rangle$ state at the target time are optimally discriminated against via destructive interference. The final residue wave function $\psi_+(t_f)$ on the $|+\rangle$ surface that satisfies $c_T(t_f) = \langle\phi_+|\psi_+(t_f)\rangle = 0$ (cf. eq 17) has actually a node at the center of target region (cf. the upper part of Figure 6). For the same reason as discussed in Figure 5, the resulting yield in the $|-\rangle$ state, i.e. $P_-(t_f) = \langle\psi_-(t_f)|\psi_-(t_f)\rangle$ (cf. the lower part of Figure 6), is quadrupled with respect to that in the individual optimal one- or three-photon process (the lower part of Figure 4).

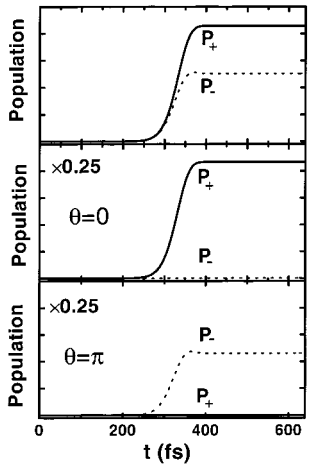

Figure 7. Evolutions of populations P_+ (solid) and P_- (dotted) on two degenerate $|+\rangle$ and $|-\rangle$ state surfaces. The upper part is for the control via the individual optimal one-photon or three-photon field (cf. Figure 4). The middle and the bottom parts result from the optimal "1+3"-coherent control with the indicated values of the additional phase θ.

Figure 7 summarizes the evolution of populations on the degenerate $|+\rangle$ and $|-\rangle$ state surfaces in the three control schemes presented respectively in Figures 4−6. Again, it demonstrates that in the weak response regime the optimal control via a single excitation pathway (the upper panel of Figure 7) is unable to achieve the selectivity between two degenerate $|+\rangle$ and $|-\rangle$ states. The optimal coherent control with two degenerate excitation pathways provides a realistic and simple scheme to achieve the desired selectivity. The maximization and the minimization of the $|+\rangle$ state product can be achieved in the optimal coherent control scheme by setting the additional phase $\theta = 0$ (the middle panel of Figure 7) and $\theta = \pi$ (the bottom panel of Figure 7), respectively.

IV. Summary and Concluding Remarks

We have developed a theory of optimal "1 + n"-coherent control that exploits the advantages of both the tailored pulses and the direct quantum interference between two degenerate optical excitation pathways. For the clarity of theoretical development, we have only considered a simplified molecular model in which there are no intermediate absorptions to compete with the direct multiphoton excitation processes. In this case, the optimal coherent control theory can be formulated analytically in terms of the individual optimal fields, their relative phase and intensity (eqs 18−20). In a general molecular system, the analytical expressions may only be obtained for the optimal "1+2"-coherent control of pure states,[61] since in this case the two-photon (pump−pump) control is an eigenvalue problem.[50,62] In the present work, the fields of individual pathways are formulated via optimal control theory (OCT) as a problem of optimization in a functional space (cf. eqs 18 and 19), while their intensities and relative phase are determined by a simple consideration of the quantum interference (cf. eqs 17, 20, and 21). It should be able to incorporate the intensities and relative

phase in the context of optimization in a parameter space.[60] A general optimal coherent control (OCC) theory based on the optimization in a joint functional and parameter space shall be formulated in future.

As a numerical demonstration we considered a wave packet focusing target with the electronic selectivity in one of two electronically degenerate states. This electronically selected phase-space target would neither be achievable via the conventional continuous-wave (cw) coherent control scheme[16−19] nor via a single optimal control field[1−3,50] in the weak response regime. In principle, the general optimal control theory in the strong response regime[1,33−36] is capable of this type of selective control. However, the resulting optimal field in the strong response regime is usually too complicated to be theoretically analyzable. The OCC scheme provides an alternative approach to this selected phase-space target product, in which the control fields are usually of simple forms and the underlying dynamic processes are often readily analyzable. One of the interesting results in the model calculation is the degenerate time-frequency coherence condition (eq 27). This result may be considered as a generalization of the degenerate excitation frequency condition (eq 16) in the conventional cw coherent control scheme. In the present simple model calculation, the control yield $|c_n(t_f)|^2$ (or the population transfer) in each individual pathway has been chosen as 2%, leading to an 8% population transfer as two optimal pathways are coherently superimposed (cf. eq 21 with $\theta = 0$). The corresponding peak power for E_3 control field is $A_3 = 3.24 \times 10^{12}$ W/cm^2 (cf. eq 26 and the comments). Although it remains in the weak three-photon response regime for the present model system, this field may strongly and resonantly couple the target state to other excited surfaces in a real molecule. To avoid the possible complication due to strong field effect, OCC with lower field intensities could be considered according to the scaling law of eq 26. However, a reduction of peak power A_3 by a factor of 10 would cost the population transfer by a factor of 10^3. Furthermore, the dispersion of an optical medium at the one-photon frequency Ω_1 is usually different from that at the three-photon frequency $\Omega_3 = \Omega_1/3$. As a result, the relative phase between two excitation pathways inside the molecular sample has a distribution. In this case, eq 21 should include an appropriate average over the θ-distribution.

Despite the simplified theoretical model and numerical examples demonstrated in this paper, the principle of OCC is general and applicable to arbitrary molecular dynamic systems. There has been much recent interest in the matter phase lag information associated with two coherent cw excitation pathways.[21−23,63−65] The optimal coherent control by two tailored light pulses may provide a mean to the study of the transient phase lag information arising from the matter wave packet dynamics. Moreover, the OCC scheme could be readily incorporated into experimental feedback-control setup with computer-based automatic pulse shapers[54−56] to control chemical selectivity.[14,53,57]

Acknowledgment. Support from the Research Grants Council of Hong Kong Government and the National Natural Science Foundation of China is gratefully acknowledged.

References and Notes

(1) Yan, Y. J.; Gillilan, R. E.; Whitnell, R. M.; Wilson, K. R.; Mukamel, S. *J. Phys. Chem.* **1993**, *97*, 2320.

(2) Krause, J. L.; Whitnell, R. M.; Wilson, K. R.; Yan, Y. J.; Mukamel, S. *J. Chem. Phys.* **1993**, *99*, 6562.

(3) Krause, J. L.; Whitnell, R. M.; Wilson, K. R.; Yan, Y. J. In *Femtosecond Chemistry*; Manz, J., Wöste, L., Eds.; VCH: Weinheim, 1995; p 743.

(4) Krause, J. L.; Schafer, K. J.; Ben-Nun, M.; Wilson, K. R. *Phys. Rev. Lett.* **1997**, *79*, 4978.

(5) Cao, J. S.; Messina, M.; Wilson, K. R. *J. Chem. Phys.* **1997**, *106*, 5239.

(6) Cao, J. S.; Bardeen, C. J.; Wilson, K. R. *Phys. Rev. Lett.* **1998**, *80*, 1406.

(7) Kohler, B.; Yakovlev, V. V.; Wilson, K. R.; Squier, J.; Delong, K. W.; Trebino, R. *Opt. Lett.* **1995**, *20*, 483.

(8) Barty, C. P. J.; Korn, G.; Raksi, F.; Rose-Petruck, C.; Squier, J.; Tien, A.-C.; Wilson, K. R.; Yakovlev, V. V.; Yamakawa, K. *Opt. Lett.* **1996**, *21*, 219.

(9) Squier, J. A.; Fittinghoff, D. N.; Barty, C. P. J.; Wilson, K. R.; Muller, M.; Brakenhoff, G. J. *Opt. Commun.* **1998**, *147*, 153.

(10) Kohler, B.; Yakovlev, V. V.; Che, J.; Krause, J. L.; Messina, M.; Wilson, K. R.; Schwentner, N.; Whitnell, R. M.; Yan, Y. J. *Phys. Rev. Lett.* **1995**, *74*, 3360.

(11) Bardeen, C. J.; Che, J.; Wilson, K. R.; Yakovlev, V. V.; Cong, P.; Kohler, B.; Krause, J. L.; Messina, M. *J. Phys. Chem. A* **1997**, *101*, 3815.

(12) Bardeen, C. J.; Che, J.; Wilson, K. R.; Yakovlev, V. V.; Apkarian, V. A.; Martens, C. C.; Zadoyan, R.; Kohler, B.; Messina, M. *J. Chem. Phys.* **1997**, *106*, 8486.

(13) Yakovlev, V. V.; Bardeen, C. J.; Che, J.; Cao, J. S.; Wilson, K. R. *J. Chem. Phys.* **1998**, *108*, 2309.

(14) Bardeen, C. J.; Yakovlev, V. V.; Wilson, K. R.; Carpenter, S. D.; Weber, P. M.; Warren, W. S. *Chem. Phys. Lett.* **1997**, *280*, 151.

(15) Gordon, R. G.; Rice, S. A. *Ann. Rev. Phys. Chem.* **1997**, *48*, 595.

(16) Brumer, P.; Shapiro, M. *Faraday Discuss. Chem. Soc.* **1986**, *82*, 177.

(17) Shapiro, M.; Brumer, P. *J. Chem. Phys.* **1986**, *84*, 4103.

(18) Shapiro, M.; Brumer, P. *Int. Rev. Phys. Chem.* **1994**, *13*, 187.

(19) Shapiro, M.; Brumer, P. *J. Chem. Soc., Faraday Trans.* **1997**, *93*, 1263.

(20) Park, S. M.; Lu, S. P.; Gordon, R. J. *J. Chem. Phys.* **1991**, *94*, 8622.

(21) Zhu, L. C.; Kleiman, V.; Li, X. N.; Lu, S. P.; Trentelman, K.; Gordon, R. J. *Science* **1995**, *270*, 77.

(22) Zhu, L. C.; Suto, K.; Fiss, J. A.; Wada, R.; Seideman, T.; Gordon, R. J. *Phys. Rev. Lett.* **1997**, *79*, 4108.

(23) Fiss, J. A.; Zhu, L.; Gordon, R. G.; Seideman, T. *Phys. Rev. Lett.* **1998**, *82*, 65.

(24) Kleiman, V. D.; Zhu, L.; Allen, J.; Gordon, R. J. *J. Chem. Phys.* **1995**, 10800.

(25) Chen, C.; Yin, Y. Y.; Elliott, D. S. *Phys. Rev. Lett.* **1990**, *64*, 507.

(26) Chen, C.; Elliott, D. S. *Phys. Rev. Lett.* **1990**, *65*, 1737.

(27) Wang, F.; Elliot, D. S. *Phys. Rev. A* **1997**, *56*, 3065.

(28) Xing, G. Q.; Wang, X. B.; Huang, X.; Bersohn, R.; Katz, B. *J. Chem. Phys.* **1996**, *104*, 826.

(29) Shnitman, A.; Sofer, I.; Golub, I.; Yogev, A.; Shapiro, M.; Chen, Z.; Brumer, P. *Phys. Rev. Lett.* **1996**, *76*, 2886.

(30) Tannor, D. J.; Rice, S. A. *J. Chem. Phys.* **1985**, *83*, 5013.

(31) Tannor, D. J.; Kosloff, R.; Rice, S. A. *J. Chem. Phys.* **1986**, *85*, 5805.

(32) Tannor, D. J.; Rice, S. A. *Adv. Chem. Phys.* **1988**, *70*, 441.

(33) Kosloff, R.; Rice, S. A.; Gaspard, P.; Tersigni, S.; Tannor, D. J. *Chem. Phys.* **1989**, *139*, 201.

(34) Peirce, A. P.; Dahleh, M. A.; Rabitz, H. *Phys. Rev. A* **1988**, *37*, 4950.

(35) Shi, S.; Woody, A.; Rabitz, H. *J. Chem. Phys.* **1988**, *88*, 6870.

(36) Rabitz, H.; Shi, S. *Adv. Mol. Vibr. Collision Dyn.* **1991**, *1A*, 187.

(37) Paramonov, G. K.; Savva, V. A. *Phys. Lett. A* **1983**, *97*, 340.

(38) Paramonov, G. K.; Savva, V. A. *Chem. Phys. Lett.* **1984**, *107*, 394.

(39) Jakubetz, W.; Just, B.; Manz, J.; Schreier, H. J. *J. Phys. Chem.* **1990**, *94*, 2294.

(40) Combariza, J. E.; Just, B.; Manz, J.; Paramonov, G. K. *J. Phys. Chem.* **1991**, *95*, 10351.

(41) Shen, H.; Dussault, J. P.; Bandrauk, A. D. *Chem. Phys. Lett.* **1994**, *221*, 498.

(42) Sugawara, M.; Fujimura, Y. *J. Chem. Phys.* **1994**, *100*, 5646.

(43) Watanabe, Y.; Umeda, H.; Ohtsuki, Y.; Kono, H.; Fujimura, Y. *Chem. Phys.* **1997**, *217*, 317.

(44) Ohtsuki, Y.; Kono, H.; Fujimura, Y. *J. Chem. Phys.* **1998**, *109*, 9318.

(45) Yan, Y. J. *J. Chem. Phys.* **1994**, *100*, 1094.

(46) Yan, Y. J.; Che, J.; Krause, J. L. *Chem. Phys.* **1997**, *217*, 297.

(47) Yan, Y. J.; Cao, J. S.; Shen, Z. W. *J. Chem. Phys.* **1997**, *107*, 3471.

(48) Yan, Y. J.; Shen, Z. W.; Zhao, Y. *Chem. Phys.* **1998**, *233*, 191.

(49) Cheng, J. X.; Shen, Z. W.; Yan, Y. J. *J. Chem. Phys.* **1998**, *109*, 1654.

(50) Yan, Y. J. *Annu. Rep. Prog. Chem., Sect. C: Phys. Chem.* **1998**, *94*, 397.
(51) Herek, J. L.; Materny, A.; Zewail, A. H. *Chem. Phys. Lett.* **1994**, *228*, 15.
(52) Schiemann, S.; Kuhn, A.; Steuerwald, S.; Bergmann, K. *Phys. Rev. Lett.* **1993**, *71*, 3637.
(53) Assion, A.; Baumert, T.; Bergt, M.; Brixner, T.; Kiefer, B.; Seyfried, V.; Strehle, M.; Gerber, G. *Science* **1998**, *282*, 919.
(54) Weiner, A. M.; Heritage, J. P.; Thurston, R. N. *Opt. Lett.* **1986**, *11*, 153.
(55) Weiner, A. M.; Heritage, J. P. *Rev. Phys. Appl.* **1987**, *22*, 1619.
(56) Weiner, A. M.; Leaird, D. E.; Patel, J. S.; Wullert II, J. R. *IEEE J. Quantum Electron.* **1992**, *28*, 908.
(57) Judson, R. S.; Rabitz, H. *Phys. Rev. Lett.* **1992**, *68*, 1500.
(58) Amstrup, B.; Tóth, G. J.; Szabó, G.; Lörincz, A. *J. Phys. Chem.* **1995**, *99*, 5206.
(59) Amstrup, B.; Doll, J. D.; Sauerbrey, R. A.; Szabó, G.; Lörincz, A. *Phys. Rev. A* **1993**, *48*, 3830.
(60) Gross, P.; Rabitz, H. *J. Chem. Phys.* **1996**, *105*, 1299.
(61) Xu, R.; Cheng, J. X.; Yan, Y. J. In preparation.
(62) Dubov, V.; Rabitz, H. *Phys. Rev. A* **1996**, *54*, 710.
(63) Seideman, T. *J. Chem. Phys.* **1998**, *108*, 1915.
(64) Nakajima, T.; Zhang, J.; Lambropoulos, P. *J. Phys. B* **1997**, *30*, 1077.
(65) Lefebvre-Brion, H. *J. Chem. Phys.* **1997**, *106*, 2544.